June 2024

Predicting pH at In-Situ Temperature for Aquatic Environments

Sarah E. Bartoloni
University of South Florida

Predicting pH at In-Situ Temperature for Aquatic Environments

by

Sarah E. Bartoloni

A thesis submitted in partial fulfillment
of the requirements for the degree of
Master of Science
with concentration in Chemical Oceanography
College of Marine Science
University of South Florida

Co-Major Professor: Robert H. Byrne, Ph.D.
Co-Major Professor: Don Chambers, Ph.D.
Kimberly Yates, Ph.D.

Date of Approval:
May 30, 2024

Keywords: CO_2 system, dissociation constants, modeling, spectrophotometry

TABLE OF CONTENTS

LIST OF TABLES

LIST OF FIGURES

ABSTRACT

pH is typically measured at a constant temperature and, as needed, converted to in-situ temperature using a system of thermodynamic equations. Using this equilibrium approach, adjustment of pH to in situ conditions requires two measured CO_2 system parameters (pH, total alkalinity, dissolved inorganic carbon, or CO_2 fugacity). Currently, when pH is the only measured CO_2 system parameter, linear models are used to adjust the pH to in-situ temperature. Although many studies have attempted to optimize CO_2 equilibrium constants (K_1 and K_2) for the CO_2 system over a range of conditions, very little prior work has experimentally examined which CO_2 system models best predict changes in pH with changing temperature ($\Delta pH/\Delta t$). In the present work, theoretical predictions of $\Delta pH/\Delta t$ are examined using CO2sys. Calculations involved the use of five different sets of dissociation constants to determine how the $\Delta pH/\Delta t$ varies with salinity (10–35) and temperature (0–40°C), for seawater whose pH measured at 25°C (pH_{25}) ranged between 7.2 and 8.2. It is shown that, in a closed system, the dependence of $\Delta pH/\Delta t$ on temperature is approximately linear, and that the dependence on salinity for open-ocean conditions is relatively weak. Notably, $\Delta pH/\Delta t$ is strongly dependent on the ratio of total alkalinity (A_T) to total inorganic carbon (C_T). The pH of a sample measured at constant temperature, such as 25°C, serves as an excellent proxy for A_T/C_T whereupon $\Delta pH/\Delta t$ can be well-modeled solely in terms of pH_{25} (i.e., pH at 25°C), temperature and salinity. It is, furthermore, demonstrated that $\Delta pH/\Delta t$ modeled in this manner is substantially independent of A_T when $1800 < A_T < 2400$ μmol kg^{-1}. In addition to theoretical models of $\Delta pH/\Delta t$ behavior, direct experimental determinations of $\Delta pH/\Delta t$ were conducted spectrophotometrically that allow

assessment of the consistency between CO2sys models and measured values over a range of salinity (10–36), temperature (15–40°C) and pH at 25°C (7.2–8.2). Finally, an improved model of $\Delta pH/\Delta t$ is presented that requires inputs of only salinity, temperature, and pH_{25}.

CHAPTER 1: PREDICTING pH AT IN-SITU TEMPERATURE FOR AQUATIC EVIRONMENTS

Introduction

Modeling in-situ pH

In laboratory and shipboard analyses, pH is typically measured at constant temperature (e.g., 25 °C, denoted pH_{25}) and, when necessary, converted to an in-situ temperature using CO_2 system solvers, such as CO2sys (Lewis & Wallace, 1998). These calculations require any two of the four main parameters that describe the marine CO_2 system: pH, dissolved inorganic carbon (C_T), total alkalinity (A_T), and CO_2 fugacity (fCO_2) plus a system of thermodynamic equations that relate the parameters. Prior studies have examined CO_2 system equilibrium models to determine which most accurately relate pH to the magnitudes of the other three parameters (Dickson & Riley, 1978; Millero, 1995; Orr et al., 2018; Woosley, 2021). This has most often been accomplished by comparing direct A_T observations with predictions of A_T calculated from C_T and pH observations under constant laboratory or shipboard temperature. A relatively underutilized form of such assessments involves the determination of pH at constant C_T and A_T over a range of temperatures. Studies of this type address a simple but fundamental question: How does temperature influence the pH of seawater? Relatively little prior work (Table 1) has been devoted to investigation of this question.

Previous studies have analyzed how seawater pH changes with temperature through determining $\Delta pH/\Delta t$, described by Equation 1:

$$\frac{\Delta pH}{\Delta t} = \frac{pH_{insitu} - pH_{measured}}{t_{insitu} - t_{measured}} \quad (1)$$

where 'measured' denotes parameters measured at laboratory temperature (often 25°C). Gieskes (1969) experimentally determined the change in seawater pH with temperature ($\Delta pH/\Delta t$) on the NBS scale as –0.0114 ± 0.001 pH units per °C. In contrast to the work of Gieskes, Ben-Yaakov (1970) concluded that $\Delta pH/\Delta t$ is not constant because it is salinity, pH, and A_T dependent. Ben-Yaakov also noted that the $\Delta pH/\Delta t$ is a nonlinear function of temperature. Millero (1979) developed a polynomial equation to describe the temperature dependence of ΔpH ($pH_{insitu} - pH_{25}$) on the seawater scale (pH_{sws}) over a range of temperatures. Millero determined that pH was essentially independent of salinity for surface ocean conditions, so salinity was not considered in the model. Millero (1995) subsequently updated the model for a wider range of conditions, including salinity and the ratio of A_T to C_T as an input parameter. Notably, Millero's (1995) model is the only empirical description of the salinity dependence of $\Delta pH/\Delta t$ thus far. Millero's model showed that pH at in-situ temperature is dependent on the state of equilibria of the carbonate system. For example, ΔpH is dependent on pH_{25} and, equivalently, on the ratio of A_T/C_T (Table 1). A limitation of Millero's 1995 equation is that it requires knowledge of three of the four CO_2 system parameters. Hunter (1998) suggested that when pH is the only known CO_2 parameter, $\Delta pH/\Delta t$ should be calculated with a CO_2 system solver by estimating A_T from salinity. Lui & Chen (2017) compiled data from six-time series characterizations of surface, open-ocean pH (on the Total pH scale), and determined an average $\Delta pH/\Delta t$ for the studied time series as –0.0151 pH units $°C^{-1}$. Lui & Chen acknowledged that $\Delta pH/\Delta t$ is a non-linear function of t, pH, S, and A_T/C_T, but indicated that $\Delta pH/\Delta t$ can be considered as a linear function for their limited

range of study. Woosley (2021) analyzed consistency between CO2sys and measured pH and found that calculations using equilibrium constants models of studies who refit data from Mehrbach et al., (1973) (Dickson & Millero (1987) and Lueker et al. (2000)) were the most internally consistent. Woosley (2021) also analyzed consistency between CO2sys calculations and measured differences in the conversion of pH between temperatures. CO2sys calculations were found to underestimate measured pH when converted to temperatures below 25°C and overestimate pH when converted to temperatures above 25°C. Finally, Hu (2022) conducted an experimental analysis of $\Delta pH/\Delta t$ using glass pH electrodes and compared the results to theoretical data, derived from CO2sys, on both the NBS and Total pH scales. Hu (2022) confirmed that $\Delta pH/\Delta t$ changes non-linearly with temperature and suggested that CO2sys should be used for adjusting pH as a function of temperature. In addition, they reported linear approximations for the influence of salinity, pH, and C_T on $\Delta pH/\Delta t$.

Previous determinations of $\Delta pH/\Delta t$ focused on theoretical models with limited experimental studies involving glass electrodes (Gieskes, 1969; Hu, 2022) that, as noted by Whitfield & Jagner, (1981), can have drifts of 0.01 pH h^{-1}. Previous studies have focused on surface open ocean conditions, with the exception of Ben–Yaakov (1970) and Hu (2022). In the present study, previous investigations are expanded upon by examining $\Delta pH/\Delta t$ predictions derived from different equilibrium models for a full range of oceanographic conditions (pH_{25}, temperature, and salinity). In addition, experimental determinations of $\Delta pH/\Delta t$ conducted using spectrophotometric procedures are compared to the predictions derived from CO2sys equilibrium models. Based on this theoretical and experimental work a model was created for calculation of $\Delta pH/\Delta t$ based solely on inputs of pH_{25} (i.e., pH measured at 25 °C), temperature, and salinity.

An explicit model that describes how pH varies with temperature will allow for direct, accurate predictions of pH at in-situ temperature when no other CO_2 system parameter is available. The model developed here can also be incorporated into climate modeling to enhance predictions of future ocean pH. $\Delta pH/\Delta t$ models are useful for correcting CO_2 data collected via autonomous platforms since pH is often the only measured CO_2 parameter. In biological or geological studies, a $\Delta pH/\Delta t$ model can be used to estimate how the pH of a given system will fluctuate over experimental or historical temperature ranges

CO_2 System Equilibria

Inorganic carbon consists of dissolved carbon dioxide (CO_2^*), bicarbonate (HCO_3^-), and carbonate (CO_3^{2-}) ions. This system is continuously exchanging H^+ ions through the following equilibria:

$$CO_2^* + H_2O \rightleftharpoons HCO_3^- + H^+ \tag{2}$$

$$HCO_3^- \rightleftharpoons CO_3^{2-} + H^+ \tag{3}$$

The stoichiometric dissociation constants for equilibria in Equations (2) and (3) are:

$$K_1 = \frac{[HCO_3^-]_T [H^+]_T}{[CO_2^*]}, \tag{4}$$

.

Table 1: Summary of previous determinations of $\Delta pH/\Delta t$. pH on the NBS, total (T), and seawater (SWS) scales are denoted by subscripts.

	Model	Method	S & t Range (°C)	Comments
Gieskes 1969	$\frac{\Delta pH}{\Delta t} = -0.0114 \pm 0.001$ pH_{NBS} units $°C^{-1}$	Theory	S: 7-35 t: 0-25	Does not report salinity influence or dependence on initial pH.
Ben–Yaakov 1970	$\frac{\Delta pH}{\Delta t} = 0.008$ to 0.0124 pH units $°C^{-1}$	Theory	S: ~5-20 t: 0-20	Reported $\Delta pH/\Delta t$ to be salinity, pH, and A_T dependent.
Millero 1979	$\Delta pH_{NBS} = A(t - 25) + B(t - 25)^2$ $A = a_0 - a_1(pH_{25} - 8) + a_2(pH_{25} - 8)^2$ $B = b_0 - b_1(pH_{25} - 8) + b_2(pH_{25} - 8)^2$ ($\sigma = 0.002$ pH units)	Theory	S: 30-40 t: 0-40	Created first non-linear model of ΔpH.
Millero 1995	$\Delta pH_{sws} = A + Bt + Ct^2$ $A = a_0 + a_1S + a_2S^2 + a_3X + a_4X^2$ $B = b_0 + b_1X + b_2X^2 + b_3S$ $C = c_0$ (Standard error = 0.003 pH units)	Theory	S: 30-40 t: 0-40	Updated model to include the dependence of ΔpH on S and the ratio of A_T/C_T (X). Requires knowledge of A_T and C_T.
Hunter 1998	Recommendation: a) Estimate A_T from salinity b) Compute C_T from A_T and pH_{25} c) Calculate pH_T using A_T and C_T (error = 0.0002 pH unit)	Theory	S: 32.5-37.5 t: 0-40	Recommends estimating A_T from S to calculate $\Delta pH/\Delta t$ when only pH is known.
Degrandpre et al. 2014	$\frac{\Delta pH}{\Delta t} = -0.015$ to -0.016 units $°C^{-1}$	Theory	S: 32, 35, 36 t: 11, 23, 25	Reported $\Delta pH/\Delta t$ values observed at the HOT, BATS, and Eastern Pacific waters (Harris et al., 2013).
Lui and Chen 2017	$\frac{\Delta pH}{\Delta t} = -0.0151$ pH_T units $°C^{-1}$ (Standard error = 0.000357 ± 0.000648)	1 Station: Spec. 5 Stations: Theory	S: Open ocean surface waters t: 1-31	Reported linear model and assumes $\Delta pH/\Delta t$ is independent of salinity for studied time series.

Table 1 : (Continued)

Woosley 2021	Assessed internal consistency of pH when converted from measured to various temperatures.	Theory and spec. pH	*S*: 33.494–33.841 *t*: -1.7–40	Assessed internal consistency of pH via. CRMs. Found pH to be more internally consistent at lower temperatures.
Hu 2022	Recommends using CO2sys to adjust the temperature of pH.	Glass electrode	S: 35, 20–105 (pH_{25} 8) *t*: 0-25, 0-40 (pH_{25} 8)	Provided averages of effects of S, initial pH, and C_T on $\Delta pH/\Delta t$. Compared experimental and theoretical data.

$$K_2 = \frac{\left[CO_3^{2-}\right]_T \left[H^+\right]_T}{[HCO_3^-]_T}, \quad (5)$$

where $[]_T$ represents the concentration of free ions plus ion pairs. At temperature 25°C and a salinity of approximately 35, pK_1 (where pK = –log$K$) is 5.847, and pK_2 is 8.971. Dissociation constants are functions of salinity and temperature; therefore, in addition to being dependent on the concentrations of species that exchange H^+ ions, pH is also salinity and temperature dependent (Ben-Yaakov, 1970; Mehrbach et al., 1973; Dickson & Millero, 1987; Millero, 1995).

Four main parameters describe the marine CO_2 system and are defined as follows:

$$A_T = [HCO_3^-]_T + 2\left[CO_3^{2-}\right]_T + [B(OH)_4^-]_T + [OH^-]_T + 2\left[PO_4^{3-}\right] + \left[HPO_4^{2-}\right] - [H^+]+... \quad (6)$$

$$C_T = \left[CO_3^{2-}\right]_T + [HCO_3^-]_T + \left[CO_2^*\right] \quad (7)$$

$$pH_T = -\log\left[H^+\right]_T \quad (8)$$

$$f(CO_2) = \frac{[CO_2^*]}{K_0} \quad (9)$$

where pH_T indicates pH on the total scale, $[]_T$ represents free plus ion-paired concentrations, $[H^+]$ is the sum of free hydrogen and bisulfate ions, and K_0 is the Henrys law constant for CO_2. Any two parameters can be used to calculate all other CO_2 system parameters through thermodynamic

equations (Park, 1969). When A_T and C_T are known, pH at in-situ conditions can be calculated via the equilibrium relationship shown below as Equation 10 (Schockman & Byrne, 2021):

$$A_T = C_T\left(\frac{2K_1K_2 + K_1[H^+]_T}{K_1K_2 + K_1[H^+]_T + [H^+]_T^2}\right) + B_T\left(\frac{K_B}{K_B + [H^+]_T}\right) + K_w[H^+]_T^{-1} - [H^+]_T + \ldots \quad (10)$$

where B_T is the total Boron concentration, K_B is the equilibrium constant of boric acid dissolution, and K_w is the dissociation constant of water. Minor terms have been omitted. Almost all CO_2 system characterizations require the use of equilibrium equations to relate in-situ conditions to measurement conditions. Formulation of a general model to explicitly express pH as a function of temperature and pH_{25} has been a sought-after goal for more than five decades and would be a valuable addition to the community, especially in cases where pH_{25} is the sole measured CO_2-system parameter.

Spectrophotometric pH Measurements

Spectrophotometric pH is based on the reaction of a sulfonephthalein indicator's (meta cresol purple (mCP)) protonated (HI^-) and unprotonated (I^{2-}) forms. Concentrations of each species are determined according Beer's law, using absorbance measurements at two wavelengths, corresponding to peak absorbances (A) of each indicator form

$$A = {}_{HI}\varepsilon b[HI^-] + {}_{I}\varepsilon b[I^{2-}]. \quad (11)$$

where $[HI^-]$ and $[I^{2-}]$ are the concentrations of the protonated and unprotonated forms of mCP, ε is the corresponding molar absorptivity form, and b is the pathlength. The ratio of absorbances of HI^- and I^{2-} is calculated according to,

$$R = \frac{A_{578} - A_{700}}{A_{434} - A_{700}}, \tag{12}$$

where A_{700} corresponds to the baseline transmittance at 700 nm. pH was calculated according Liu et al. (2011),

$$\mathrm{pH_T} = -\log\left(K_2^{\mathrm{T}} e_2\right) + \log\left(\frac{R - e_1}{1 - R\frac{e_3}{e_2}}\right) \tag{13}$$

where K_2^{T} is the dissociation constant of the HI^-, and e_1, e_2, and e_3 are the molar absorptivity ratios of the indicator.

Methods

Overview

CO2sys, experimental analysis, and models were used to analyze, measure, and predict $\Delta pH/\Delta t$. CO2sys was used to observe how $\Delta pH/\Delta t$ varies with in-situ temperature, pH_{25}, and salinity. Various equilibrium constant determinations were used to predict $\Delta pH/\Delta t$ in CO2sys to discern the impact of the choice of constants in $\Delta pH/\Delta t$ calculations. Next, $\Delta pH/\Delta t$ was experimentally determined to compare CO2sys predictions to measured values. Through experimental comparison, the equilibrium constant determination that predicts the most accurate

$\Delta pH/\Delta t$ relative to experimental results can be discerned. Finally, a model was produced to predict $\Delta pH/\Delta t$ based information acquired in CO2sys and experimental analysis.

Chemicals

Seawater was collected offshore on the Southwest Florida Shelf, in the Gulf of Mexico. The seawater pH was adjusted using aliquots of 1 N HCl (Fisher Chemical, CAS 7647-01-0) or 1 N NaOH (Fisher Chemical, CAS 1310-73-2). Meta-cresol purple (mCP) (10mM in 0.7 M NaCl), purified at the University of South Florida according to Liu et al. (2011), was used in all spectrophotometric pH measurements.

Equipment

All experimental pH measurements were conducted using an Agilent Cary 60 UV-Vis spectrophotometer and 10 cm optical glass spectrophotometric cells. Salinity was measured with a Guildline Portasal salinometer (Model 8410). A_T was measured using a USB4000 Fiber Optic Spectrometer (Ocean Optics) with the indicator dye bromocresol purple (BCP) and methods from Liu et al., 2015. A_T measurements were calibrated daily with certified reference materials (CRM; batch numbers 187 & 201) prepared at the Scripps Institution of Oceanography of the University of California, San Diego.

A circulating water bath was used to control the temperature of the water-jacketed holder of the spectrophotometric cell (Thermo Scientific NESLAB RTE-7). Additions of mCP were made using a 2 mL Gilmont micrometer buret (GS-1200). A hole was drilled through the center of a Teflon cap to fit a mini surface temperature sensor (Vernier STS-BTA). The cap and sensor were sealed with epoxy. This modification allowed the temperature sensor to measure in-situ

temperature of the seawater inside the spectrophotometric cell throughout the experiment. The accuracy and resolution of the temperature sensor is ± 0.2°C and 0.03°C respectively. A quartz thermometer (Hewlett Packard Model 2804 A) was used to calibrate the temperature sensor periodically, thereby improving its accuracy. Experiments were conducted to establish that the modified spectrophotometric cell cap was impermeable to CO_2 over the course of the experiment. The temperature of the system was heated in a stair-like pattern, with intermitant periods of increasing and holding cell temperature. This heating pattern allowed the spectrophotometric cell to be uniformly heated and resulted in a homogenous sample temperature.

CO2sys Calculations

All theoretical pH and $\Delta pH/\Delta t$ values were calculated using PyCO2SYS v1.8 (hereby referred to as CO2sys) (Humphreys et al., 2022). Total alkalinity was assumed to be 2000 µmol kg^{-1} for all calculations unless stated otherwise. Values of $KHSO_4$, KHF, and the total Boron concentration were used from Dickson, 1990, Dickson & Riley, 1979, and Lee et al., 2010 respectively. All pH and $\Delta pH/\Delta t$ values are reported on the total pH scale.

Predictions of pH over a range of temperatures were calculated at constant A_T (2000 µmol kg^{-1}) and C_T (1950 µmol kg^{-1}) using CO2sys. pH predictions were calculated in CO2sys for salinities 10–35 using five different equilibrium constant algorithms (Lueker et al., 2000; Roy et al., 1993; Schockman & Byrne, 2021; Sulpis et al., 2020; Waters et al., 2014). Calculations were limited by the different temperature and salinity ranges of the published equilibrium constants.

CO2sys was used to determine $\Delta pH/\Delta t$ as a function of temperature by calculating $\Delta pH/\Delta t$ over 1° temperature increments, spanning from 0–40°C. $\Delta pH/\Delta t$ was calculated at

different pH_{25} values (7.2–8.2) and salinities (10, 20, 30, 36). To calculate $\Delta pH/\Delta t$, a starting A_T (2000 μmol kg^{-1}) and pH_{25} value were defined, and the C_T of the system was thereby determined using CO2sys. pH at various temperatures was then calculated from A_T and C_T according to Equation 10. Temperature was incremented by 1°C, spanning the temperature and salinity ranges corresponding to each equilibrium constant determination.

CO2sys was used to determine $\Delta pH/\Delta t$ as a function of pH_{25}. To achieve this, $\Delta pH/\Delta t$ was calculated for a 1°C increment of temperature at 5, 15, 25, and 35°C (referred to as reference temperatures). The change in pH (ΔpH) was calculated as the difference between pH at ± 0.5°C of the reference temperature, and was calculated over a range of pH_{25} values (7.2–8.2). For example, $(\Delta pH/\Delta t)_{25}$ analyzes the change in pH between 24.5 and 25.5°C. The change in pH with a 1°C increment will be referred to as $(\Delta pH/\Delta t)_t$, where the subscript t denotes the reference temperature. Calculations were performed by first calculating C_T from starting pH_{25} (7.2–8.2) and A_T (1800, 2000, 2400 μmol kg^{-1}) values. A_T and calculated C_T were then used to calculate pH at ± 0.5°C of the reference temperature (ie. 24.5 and 25.5 °C) and $(\Delta pH/\Delta t)_t$ was then calculated using the differences in pH and temperature. This method was repeated for salinities 10, 20, 30, and 36.

Spectrophotometric determinations of $\Delta pH/\Delta t$

Spectrophotometric measurements of pH were made following methods developed by Clayton & Byrne (1993). One deviation from these methods was made; 700 nm was used as the non-absorbing wavelength of mCP instead of 730 nm. Typically, the pH of a sample is measured at one temperature, therefore only one background reference is required. Here, the real-time change in pH with temperature was measured, therefore the pH of a single sample was recorded

at multiple temperatures. The absorbance of water is temperature dependent at the standard background wavelength (730nm) (Pegau et al., 1997). A new background wavelength of 700 nm was chosen because the absorbance of water is not temperature dependent at this wavelength and 700 nm is outside the absorbance range of mCP (Liu et al., 2011). Absorbance measurements (collected at 434 and 578 nm) were first obtained at 25°C. Purified mCP (10 µL) was then added to the cell containing seawater and absorbances were recorded. The temperature of the system was then decreased to ~15°C and raised to 40°C. Temperature was recorded once every second and the absorbance was obtained every 30 seconds. Small baseline corrections were made to the absorbances using the non-absorbing wavelength. Seawater pH (total scale) was calculated using a ratio of 578 and 434 nm through the mCP parametrization of Müller & Rehder (2018).

The change in pH with changing temperature was determined spectrophotometrically for a pH_{25} range of 7.2–8.2, a temperature range of 15–40°C and salinities 10.1, 20.2, 30.2, and 36.1. Experimentally determined $\Delta pH/\Delta t$ was directly compared to predicted values, for all equilibrium constant determinations, by using experimental values of pH at 25°C, temperature, salinity, and measured A_T as input parameters in CO2sys. Consistency was assessed by calculating the difference in experimental (measured) and CO2sys (calculated) pH.

Results and Discussion

CO2sys Predictions

At constant CO_2 system conditions (e.g., A_T = 2000 µmol kg^{-1} and C_T = 1950 µmol kg^{-1}) pH is strongly influenced by temperature and significantly influenced by salinity, as shown in Figure 1. All equilibrium constant models predict changes in pH with temperature that exhibit only minor deviations from linearity. Despite the similar trends between equilibrium constant

models, differences in predicted pH can be significant. At salinity 10, the maximum difference between pH calculated using constants of Roy et al., 1993 and Waters et al., 2014 is 0.040 pH units. At salinity 35, equilibrium constant calculations using constants from Roy et al., 1993 and Sulpis et al., 2021 differ by a maximum of 0.033 pH units. The choice of which equilibrium constant determinations to use in CO2sys calculations of pH can greatly impact final results.

It is difficult to effectively differentiate equilibrium constant predictions in Figure 1, but model differences are easier to discern by examining first derivatives of pH as a function temperature relative to varying pH_{25} (Figure 2) and in-situ temperature conditions (Figure 3). Figure 2 examines how changes in the acid/base characteristics of the CO_2 system impact predictions of $\Delta pH/\Delta t$ over a range of pH_{25} conditions (i.e., $(\Delta pH/\Delta t)_{25}$ as a function of pH_{25}). The pH_{25} of the system is varied at a constant A_T which is equivalent to varying C_T or the A_T/C_T ratio at constant A_T. For salinities between 30 and 35, and CO_2 system conditions representative of the surface ocean, $\Delta pH/\Delta t$ values are on the order of 0.015 pH units $°C^{-1}$. All equilibrium constant models predict that $(\Delta pH/\Delta t)_{25}$ becomes increasingly negative with increasing pH_{25} (Figure 2). This behavior is attributable to differences in the thermodynamic behavior of the buffers that control seawater pH. At low pH the dominant pH buffer of seawater is HCO_3^-/CO_2* corresponding to K_1 and, at high pH, seawater is dominantly buffered by HCO_3^-/CO_3^{2-} which corresponds to K_2. Because the bicarbonate/carbonate buffer has a much larger temperature dependence than the bicarbonate/CO_2* buffer, the influence of temperature on seawater pH steadily increases with increasing pH_{25} and, equivalently, increases with increasing A_T/C_T. Accordingly, the pH of surface seawater is much more strongly dependent on temperature than the pH of seawater at depth. All equilibrium constant models strongly agree in their calculations of how $\Delta pH/\Delta t$ changes with pH_{25} conditions. Calculations using constants from Lueker et al. (2000), Waters et

al. (2014), and Schockman & Byrne (2021) have significant overlap in their calculations. Roy et al. (1993) consistently predicts the smallest values of $\Delta pH/\Delta t$ while Sulpis et al. (2020) consistently predicts the largest values. The difference between equilibrium constant models is largest at salinity 10.

Figure 3 examines how $\Delta pH/\Delta t$ changes with varying in-situ temperature conditions. Equilibrium constant models have less agreement in how $\Delta pH/\Delta t$ varies with in-situ temperature conditions (Figure 3) compared to varying pH_{25} conditions (Figure 2). With the exception of Schockman & Byrne (2021), all models predict $\Delta pH/\Delta t$ to increase with increasing temperature. Although Lueker et al. (2000), Waters et al. (2014), and Schockman & Byrne (2021) have good agreement in the absolute magnitude of the range of $\Delta pH/\Delta t$ (i.e., the first derivative of the Figure 1 plots with respect to temperature), but the slope of $\Delta pH/\Delta t$ for Schockman & Byrne (i.e., the second derivative with respect to temperature) differs in its sign. The source of the opposing slope of Schockman & Byrne (2021) in Figure 3 is unknown but it should be noted that Schockman & Byrne (2021) is currently the only model to determine K_2 using updated spectrophotometric methods. As observed in Figure 2, Roy et al. (1993) generally predicts the lowest $\Delta pH/\Delta t$ values in Figure 3 while Sulpis et al. (2020) generally predicts higher $\Delta pH/\Delta t$ values relative to other models. All $\Delta pH/\Delta t$ predictions generally decrease with increasing salinity and the largest variance between models is observed at salinity 10.

Given the good general agreement in the model predictions of Lueker et al. (2000), Waters et al. (2014), and Schockman & Byrne (2021) in Figures 1–3, averaged $\Delta pH/\Delta t$ predictions of these models are shown in Figure 4 over a salinity range of 20–30 and at pH_{25} values of 7.2, 7.6, and 8.0 (an expanded pH_{25} range is depicted in App. A Figure A1). Figure 4 combines the influence of varying pH_{25}, temperature, and salinity on $\Delta pH/\Delta t$ predictions into one

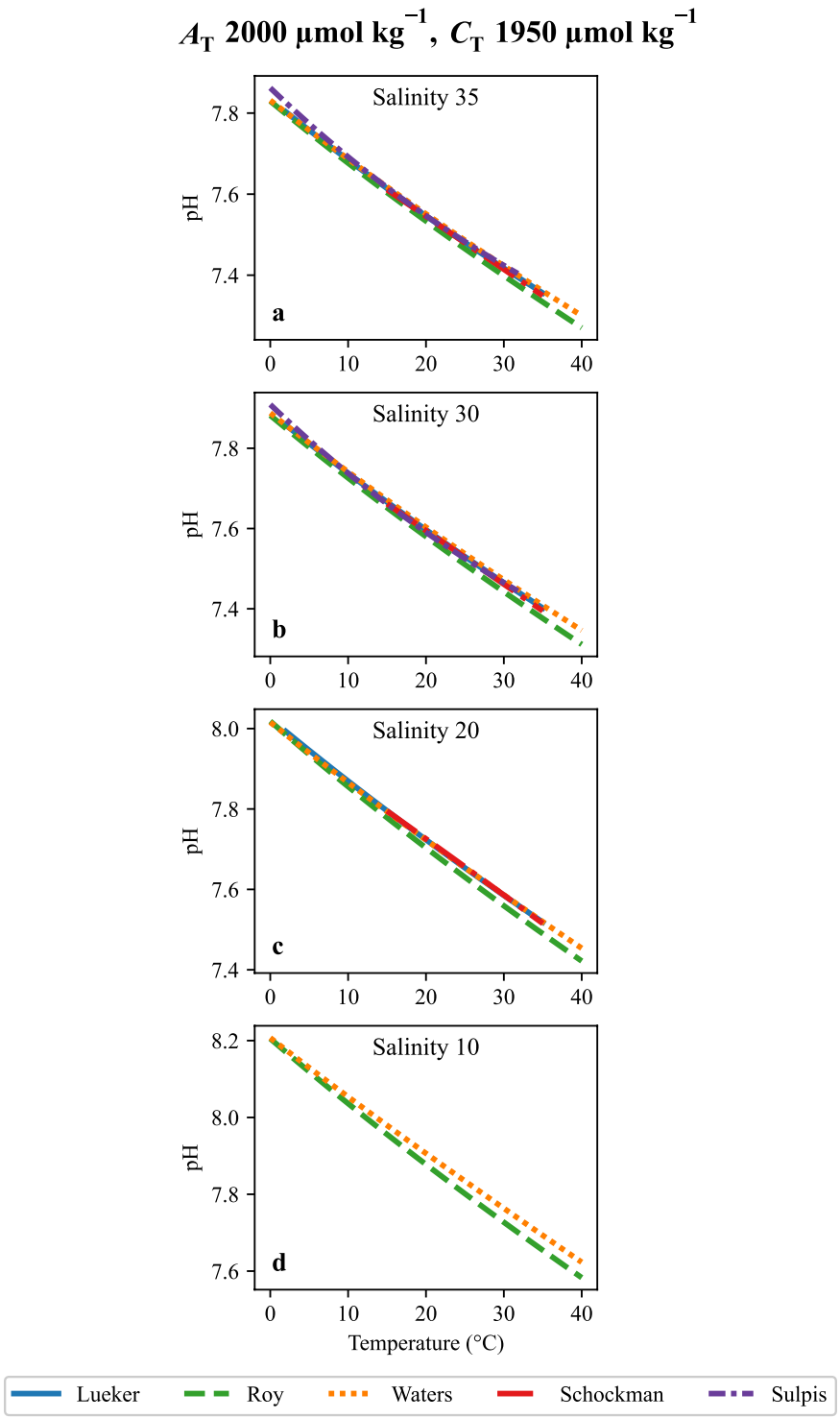

Figure 1: pH as a function of temperature as predicted by different equilibrium constants in CO2sys. pH was calculated at constant A_T (2000 µmol kg^{-1}) and C_T (1950 µmol kg^{-1}) for salinities 35 (a), 30 (b), 20 (c), and 10 (d). Note, Sulpis et al. (2020) is defined for salinities 30.73–37.57, therefore calculations of Sulpis in (b) are determined at a salinity of 30.73.

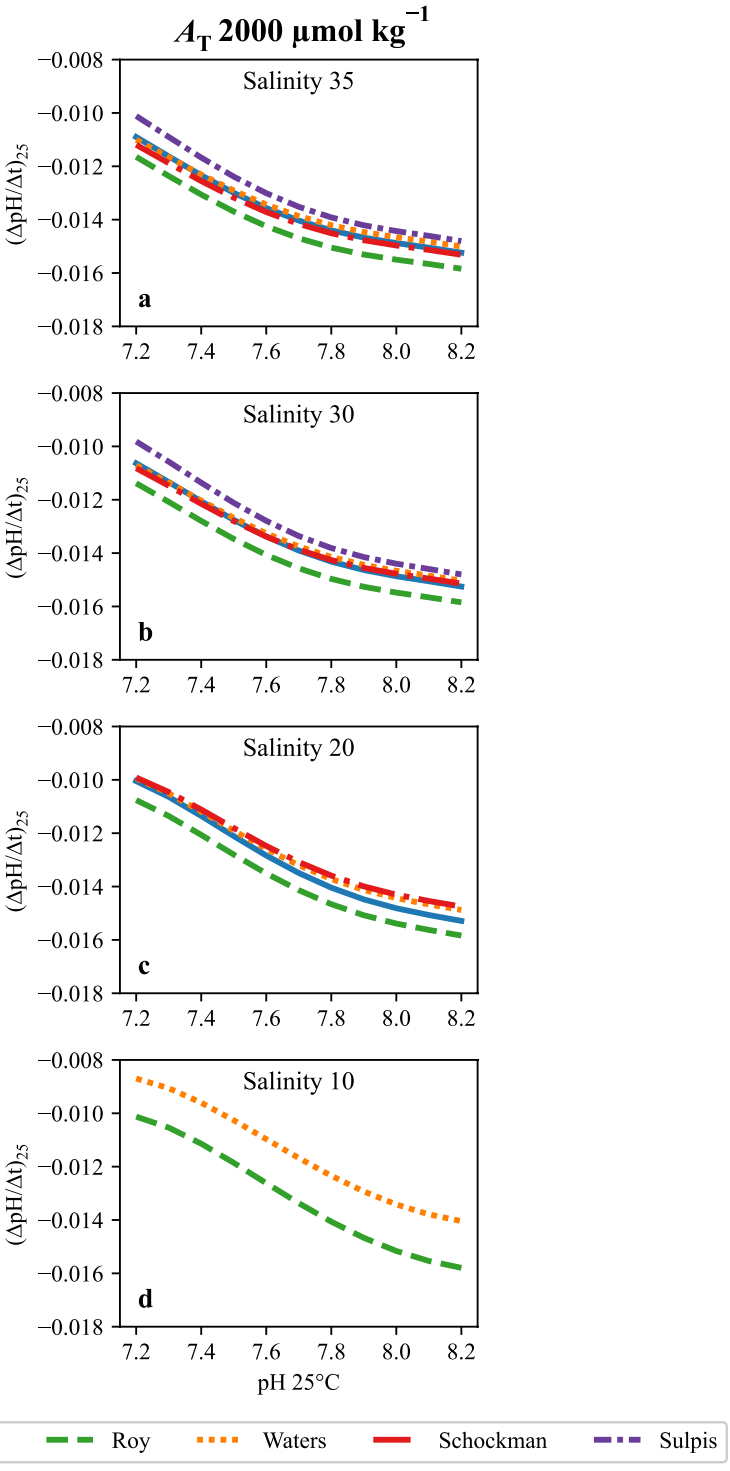

Figure 2: CO2sys predictions of $(\Delta pH/\Delta t)_{25}$ as a function of pH_{25} for different equilibrium constant models. $(\Delta pH/\Delta t)_{25}$ denotes the change in pH between temperatures 24.5 and 25.5°C. Calculations were performed in CO2sys at an A_T = 2000 µmol kg^{-1}. Note, Sulpis et al. (2020) is defined for salinities 30.73–37.57, therefore calculations of Sulpis in (b) are determined at a salinity of 30.73.

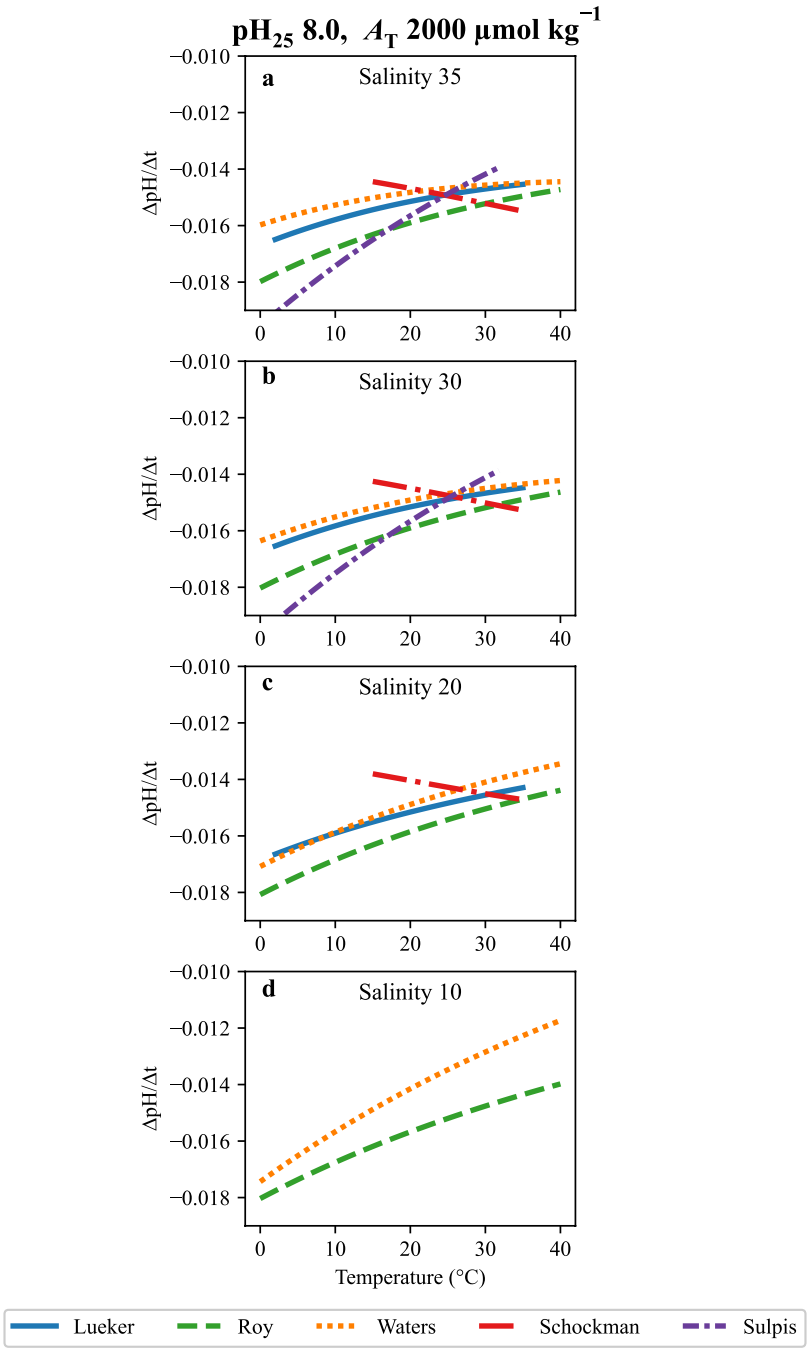

Figure 3: Comparison of $\Delta pH/\Delta t$ as a function of temperature for different equilibrium constant models. Calculations were performed using CO2sys. CO_2 system conditions were pH_{25} = 8.0 and A_T = 2000 µmol kg^{-1}, and salinities were 35 (a), 30 (b), 20 (c), and 10 (b). Note, Sulpis et al. (2020) is defined for salinities 30.73–37.57, therefore calculations of Sulpis in (b) are determined at a salinity of 30.73.

figure. At low pH_{25} conditions and high in-situ temperatures, $\Delta pH/\Delta t$ predictions are more dependent on salinity which is seen by a larger spread of calculated $\Delta pH/\Delta t$ values. At higher pH_{25} and lower temperature conditions, the influence of salinity is lower as there is stronger agreement in the values of $\Delta pH/\Delta t$ at various salinities. Figure 4 can be used to argue that pH_{25}, temperature, and salinity all greatly influence how pH changes with temperature ($\Delta pH/\Delta t$) and should all be included when creating models to predict $\Delta pH/\Delta t$ for various ocean conditions.

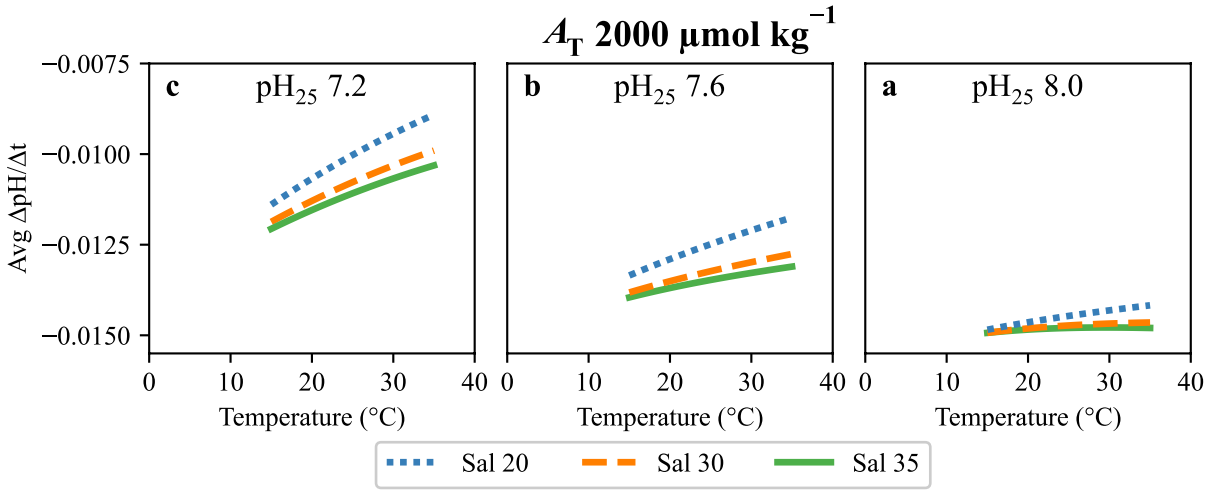

Figure 4: Averaged $\Delta pH/\Delta t$ predictions of Lueker et al. (2000), Waters et al. (2014), and Schockman & Byrne (2021) models as a function of temperature. Averaged $\Delta pH/\Delta t$ values are shown at salinities 20–35 and for pH_{25} values of 8.0 (a), 7.6 (b), and 7.2 (c). CO_2 system calculations were performed at A_T = 2000 µmol kg^{-1}.

To expand the applicability of the reported CO2sys analysis of $\Delta pH/\Delta t$, the impact of varying A_T and reference temperature conditions were also studied. $\Delta pH/\Delta t$ was found to be dependent on the acid/base characteristics of the CO_2 system by varying pH_{25} at a constant A_T (2000 µmol kg^{-1}) in Figures 2 and 4. The extent to which $(\Delta pH/\Delta t)_t$ calculations are dependent on A_T was explored over a range of 1800–2400 µmol kg^{-1} (App. A. Figure A2). Varying A_T within the studied range caused a maximum pH change of –0.00013 pH units °C^{-1} (a 0.8 % decrease).

As such, varying A_T from 1800–2400 μmol kg^{-1} does not substantially impact CO2sys calculations of $\Delta pH/\Delta t$, whereby $\Delta pH/\Delta t$ can be assumed to be independent of A_T under the investigated conditions. Previous studies have predominantly generated models to predict $\Delta pH/\Delta t$ using laboratory pH measurements and a reference temperature of 25°C (Millero, 1979, 1995). Recent studies have explored lowering the reference temperature at which pH is measured (Woosley, 2021; Carter et al., 2024). Here, the change in $\Delta pH/\Delta t$ with changing reference temperatures was examined and it was determined that applying models that utilize pH measured alternatively at 25°C or 20°C (i.e., pH_{25} and pH_{20}) introduces minimal error, with the except of Sulpis et al. (2020) (App. A. Figure A3).

Experimental Determinations of $\Delta pH/\Delta t$

Figure 5 compares experimental observations of pH at various in-situ temperature conditions with predictions using CO2sys over a temperature range of 15–35°C. Comparisons over a wider temperature and salinity range are shown in App. A, Figure A4. In agreement with the findings of Woosley (2021), CO2sys calculations were found to underestimate measured pH at temperatures below 25°C and overestimate measured pH at temperatures above 25°C, for all equilibrium constant models (at salinities 20–36) with the exception of Roy et al. (1993). Agreement with observations using the predictive models of Lueker et al. (2000), Waters et al. (2014), and Schockman & Byrne (2021) improved with decreasing pH_{25}, while those of Roy et al. (1993) and Sulpis et al. (2020) decreased. The Lueker et al. (2000) and Waters et al. (2014) models showed the best agreement with observations at salinity 20 (Figure 5 (b, f, and j)), while Roy et al. (1993) and Schockman & Byrne (2021) had the best agreement at salinity 36 (Figure 5

(d, h, and l)). Overall, these results reveal significant inconsistencies between experimental observations and CO2sys predictions.

The best agreement between experimental and modeled pH at in-situ temperature was obtained using the equilibrium constants models of Lueker et al. (2000) over the studied temperature and salinity range. Calculated pH using the Lueker et al. (2000) model had almost no deviation from experimental pH at salinity 20 (Figure 5 (b, f, and j)) and consistently had the smallest deviations from experimental pH at salinities 30 and 36. Woosley et al., 2021 also concluded that Lueker et al. (2000) and other models derived from the data of Merbach et al. (1973), have the strongest consistency with measured pH. When using CO2sys to calculate $\Delta pH/\Delta t$ choosing equilibrium constants of Lueker et al., (2000) produces the most accurate results relative to the experimental data reported here (Figure 5).

In Figure 6, the results of experimental minus CO2sys-predicted pH are averaged using the models of Lueker et al. (2000), Waters et al. (2014), and Schockman & Byrne (2021) for salinities 20–36. Figure 6 highlights that the difference between experimental and CO2sys predicted pH increases with increasing pH_{25} (App. A. Figure A5 shows full pH_{25} range). As previously mentioned, the CO_2 system is dominated by the equilibrium constant K_2 at high pH_{25} conditions. There is much more uncertainty in the current characterizations of pK_2 ($pK = -\log K$) relative to pK_1, approximately 0.02 and 0.01 respectively. Higher uncertainties in K_2 determinations may account for the larger differences between experimental and CO2sys predicted pH seen at higher pH_{25} conditions. At pH_{25} of 8.0, a negative slope is observed as a result of CO2sys underestimating pH below 25°C and overestimating pH above 25°C. As pH_{25} decreases, the slope of the residuals decreases until they are nearly flat at a pH_{25} of 7.2. The negative slope of the residuals is most prominent at salinity 36 and is reduced with decreasing

salinity. The standard deviation between averaged differences between experimental pH and CO2sys pH decreases with decreasing pH_{25}, especially for temperatures below 25°C.

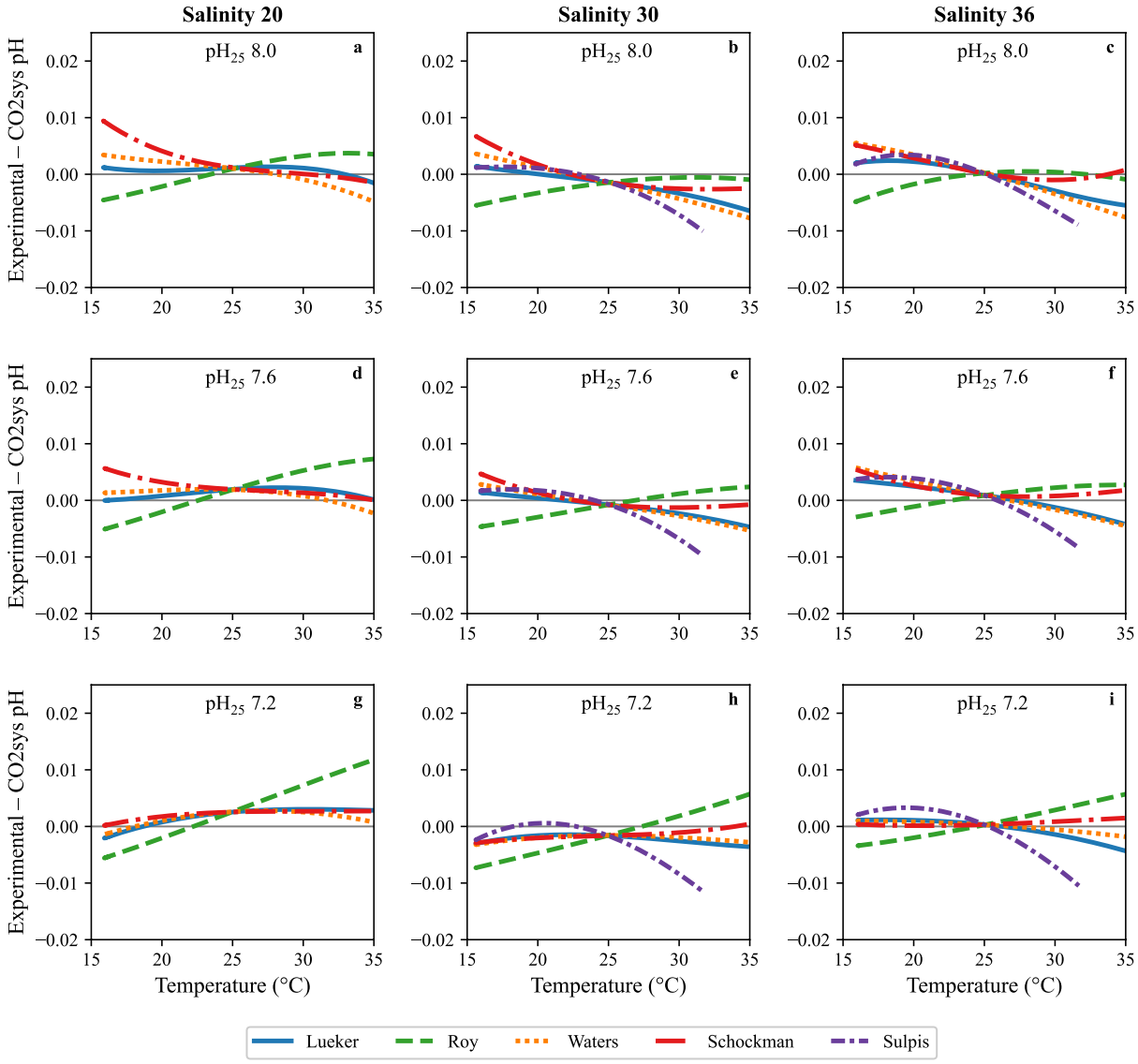

Figure 5: Consistency between experimental and CO2sys predicted pH at pH_{25} values of 8.0 (a–c), 7.6 (d–f), and 7.2 (g–i) and salinities of 20, 30, and 36 (columns moving left to right). All CO2sys predictions were calculated using exact experimental temperature, pH_{25}, salinity, and A_T. A pH difference of zero is represented by solid black lines. Note, Sulpis et al. (2020) is defined for salinities 30.73–37.57, therefore calculations of Sulpis in (c, g, k, and o) are determined at a salinity of 30.73.

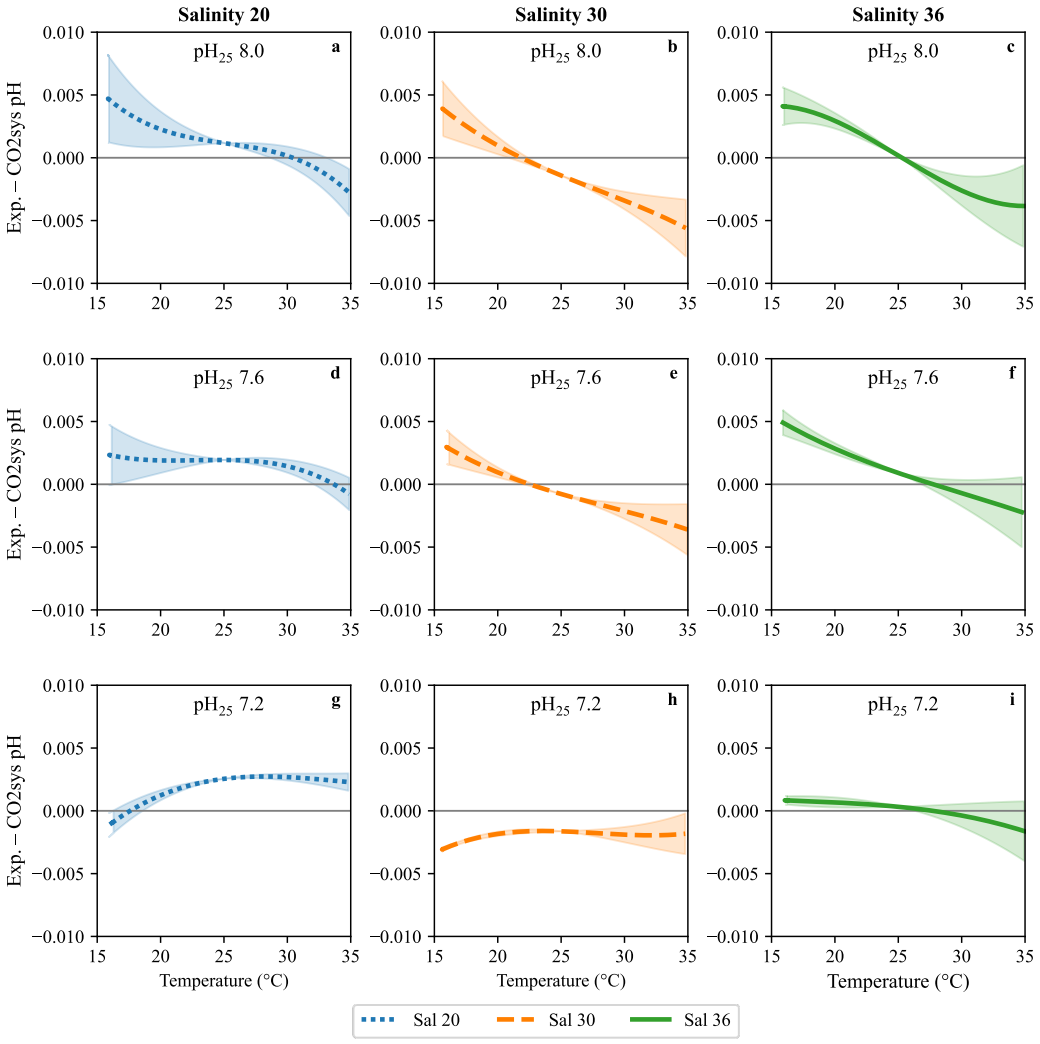

Figure 6: Difference between experimental and averaged CO2sys predictions of Lueker et al. (2000), Waters et al. (2014), and Schockman & Byrne (2021) models at pH_{25} values of 8.0 (a-c), 7.6 (d-f), and 7.2 (g-i) and salinities of 20, 30, and 36 (columns moving left to right). Shaded areas represent 1 standard deviation. All CO2sys predictions were calculated using exact experimental temperature, pH_{25}, salinity, and A_T. A pH difference of zero is represented by solid black lines.

Modeling $\Delta pH/\Delta t$

Based on CO2sys calculations and direct experimental determinations of $\Delta pH/\Delta t$, a model was developed to predict pH at in-situ temperature when pH at 25°C (pH_{25}) is the only known CO_2 system parameter for $19 < S < 43$ and $2 < t < 35$°C:

$$pH_{insitu} = pH_{25} + (t - t_{25})\left[a + b(pH_{25}) + c\left(pH_{25}^2\right) + d(t) + e\left(pH_{25} \cdot t\right) + f(S) + g\left(S \cdot pH_{25}\right)\right], \quad (12a)$$

where t is the in-situ temperature and a–f are coefficients shown in Table 2. The new model was fit to CO2sys calculations using equilibrium constants from Lueker et al. (2000), which was determined to have the best consistency relative to spectrophotometric pH measurements (Figure 5) and covered a larger temperature range compared to the presented experimental dataset. Equation 12 can also be rearranged in terms of $\Delta pH/\Delta t$ (defined by Equation 1), where

$$\frac{\Delta pH}{\Delta t} = \left[a + b(pH_{25}) + c\left(pH_{25}^2\right) + d(t) + e\left(pH_{25} \cdot t\right) + f(S) + g\left(S \cdot pH_{25}\right)\right]. \quad (12b)$$

Equation 12a and 12b are interchangeable and will be hereby be referred to as Equation 12.

The new model to predict $\Delta pH/\Delta t$ significantly expands the salinity and pH range in which pH_{insitu} and $\Delta pH/\Delta t$ can be calculated when pH is the only known CO_2 parameter. If users have a laboratory pH sample measured at 25°C, Equation 12 can be used to calculate pH at any in-situ temperature within the limitations of the Lueker et al. (2000) study ($2 < t < 35$°C, $19 < S < 43$). The new model was assessed by directly comparing modeled $\Delta pH/\Delta t$ to CO2sys predictions using equilibrium constants from Lueker et al. (2000) (App. A. Figure A6). The average difference between modeled and CO2sys calculated $\Delta pH/\Delta t$ was $5.3 \times 10^{-21} \pm 8.9 \times 10^{-5}$. For the modeled residuals, 95% had a percent error less than 1% and 99% percent had an error less than 2%. All residuals of $\Delta pH/\Delta t$ relative to CO2sys predictions were below ±0.0004 pH units. It is also important to note that the simplicity of Equation 12 was prioritized over complete randomization of its residuals. More complex models of $\Delta pH/\Delta t$ based on experimental and CO2sys calculations

Table 2: Coefficients for Equation 12.

	Coefficients for Lueker et al. Model
a	0.23720
b	–0.059486
c	3.488×10^{-3}
d	-3.987×10^{-5}
e	3.469×10^{-4}
f	-5.602×10^{-4}
g	6.952×10^{-5}

using the constants of Lueker et al. (2000) and Waters et al. (2014) are documented in Appendix A. (Equations A1–3, Figures A8–10, Table A2). In Figure 7, Equation 12 is directly compared to the most recent empirical model presented in Lui & Chen (2017) at salinity 35 and a pH_{25} range of 7.2–8.2. The residual sum of squares (RSS) for Lui & Chen's model relative to CO2sys predictions (constants from Lueker et al., 2000) was 50 times larger than the RSS of the new model. Even in open ocean conditions, the new model better predicts the dependence of $\Delta pH/\Delta t$ on t and pH_{25}.

Coefficients for Equation 12 (Table 2) were estimated using CO2sys predictions (constants from Lueker et al. (2000)) instead of experimental $\Delta pH/\Delta t$ determinations due to the limited range of experimental temperatures (15–40°C). A second set of coefficients were

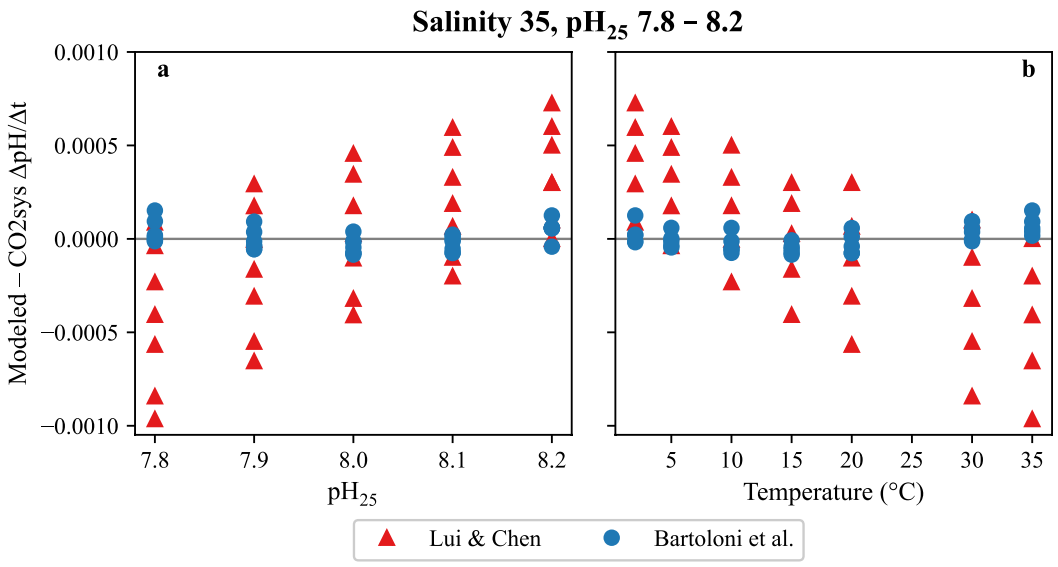

Figure 7: Residuals of modeled ΔpH/Δ*t* minus CO2sys predicted values (constants from Lueker et al. (2000)) using models of Lui & Chen (2011) (red triangles) and the model proposed in this study (blue circles, Equation 12). Residuals are compared at salinity 35, pH_{25} (a), and in-situ temperature (b).

estimated for Equation 12 using experimental data (App. A, Table A1) and used to assess the validity of Equation 12 when applied to experimental data (App. A, Figure A7). The standard deviation of residuals for Equation 12 are 2–2.7 times larger when using coefficients fit to experimental data compared to CO2sys generated data (App. A, Table A3). This indicates that Equation 12 is slightly biased towards CO2sys data and true residuals may be higher than depicted in App. A, Figure A6. Future work should focus on determining ΔpH/Δ*t* over a larger salinity and temperature range to reduce model residuals.

Equation 12 significantly improves the ability to predict pH at in-situ temperature when pH is the only known CO_2 system parameter. The new model only requires input variables of measured pH, temperature, and salinity. When laboratory or shipboard pH measurements are made between 20–25°C, the new model can be used to convert pH to in-situ conditions within the range $19 < S < 43$ and $2 < t < 35$°C. The new model summarizes the intricate salinity,

temperature, and pH dependencies of $\Delta pH/\Delta t$ while greatly expanding the salinity and pH_{25} range within which $\Delta pH/\Delta t$ can be predicted.

Conclusions

In a closed system, the dependence of seawater pH on temperature is strongly linear and only weakly dependent on salinity. The derivative of pH with temperature, $\Delta pH/\Delta t$, is well-described in terms of pH_{25} (pH at 25°C) which serves a proxy for the ratio of A_T to C_T. The five CO_2–system equilibrium constant models analyzed here had unique distinctions between the slopes of $\Delta pH/\Delta t$ with changing temperature but exhibited a strong consensus on how $\Delta pH/\Delta t$ varies with pH_{25}. Through experimental determinations of $\Delta pH/\Delta t$, CO2sys was found to somewhat overestimate in-situ pH as the temperature decreased to values below 25°C and underestimate in-situ pH as the temperature rose above 25°C. CO2sys calculations of $\Delta pH/\Delta t$ using constants from Lueker et al., 2000 had the best agreement with experimental results for salinities 20–36. $\Delta pH/\Delta t$ can be well-modeled using only pH_{25}, temperature, and salinity. The updated model produced in this work improves the simplicity and accuracy of $\Delta pH/\Delta t$ predictions while also expanding the applicable ranges of salinity (19–43) and pH_{25} (7.2–8.2) ranges.

REFERENCES

Ben-Yaakov, S. (1970). A method for calculating the in situ pH of seawater. *Limnology and Oceanography, 15*(2), 326–328. doi: 10.4319/lo.1970.15.2.0326

Clayton, T. D., & Byrne, R. H. (1993). Spectrophotometric seawater pH measurements: total hydrogen ion concentration scale calibration of m-cresol purple and at-sea results. *Deep-Sea Research: Instruments and Methods, 40*(10), 2115-2129. doi: 10.1016/0967-0637(93)90048-8

Degrandpre, M. D., Spaulding, R. S., Newton, J. O., Jaqueth, E. J., Hamblock, S. E., Umansky, A. A., Harris, K. E. (2014). Considerations for the measurement of spectrophotometric pH for ocean acidification and other studies. *Limnology and Oceanography Methods, 12*(12), 830–839. doi: 10.4319/lom.2014.12.830

Dickson, A. G. (1990). Standard potential of the reaction: AgCl(s) + 1/2H2(g) = Ag(s) + HCl(aq), and the standard acidity constant of the ion HSO4- in synthetic seawater from 237.15 to 318.15 K. *J. Chem. Thermodynamics, 22*(2), 113-127. doi: 10.1016/0021-9614(90)90074-Z

Dickson, A. G., & Millero, F. J. (1987). A comparison of the equilibrium constants for the dissociation of carbonic acid in seawater media. *Deep-Sea Research, 34*(10), 1733-1743. doi: 10.1016/0198-0149(87)90021-5

Dickson, A. G., & Riley, J. P. (1978). The effect of analytical error on the evaluation of the components of the aquatic carbon-dioxide system. *Marine Chemistry, 6*(1), 77-85. doi: 10.1016/0304-4203(78)90008-7

Dickson, A. G., & Riley, J. P. (1979). The estimation of acid dissociation constants in seawater media from potentiometric titrations with strong base. *Marine Chemistry, 7*(2), 89-99. doi: 10.1016/0304-4203(79)90001-X

Gieskes, J. M. (1969). Effect of temperature on the pH of seawater. *Limnology and Oceanography*, *14*(5), 679–685. doi: 10.4319/lo.1969.14.5.0679

Hu, Y. (2022). Temperature coefficient of seawater pH as a function of temperature, pH, DIC and salinity. *Acta Oceanologica Sinica*, *41*(6), 114–118. doi: 10.1007/s13131-021-1955-3

Humphreys, M. P., Schiller, A. J., Sandborn, D. E., Gregor, L., Pierrot, D., van Heuven, S. M. A. C., Lewis, E. R., & Wallace, D. W. R. (2022). PyCO2SYS: marine carbonate system calculations in Python. *Zenodo*.

Hunter, K. A. (1998). The temperature dependence of pH in surface seawater. *Deep-Sea Research I, 45*(11), 1919-1930. doi: 10.1016/S0967-0637(98)00047-8

Lee, K., Kim, T. W., Byrne, R. H., Millero, F. J., Feely, R. A., & Liu, Y. M. (2010). The universal ratio of boron to chlorinity for the North Pacific and North Atlantic oceans. *Geochimica et Cosmochimica Acta*, *74*(6), 1801–1811. doi: 10.1016/j.gca.2009.12.027

Lewis, E., & Wallace, D. W. R. (1998). *Program Developed for CO2 System Calculations*. ORNL/CDIAC-105, Carbon Dioxide Information Analysis Center. doi:10.2172/639712

Liu, X., Byrne, R. H., Lindemuth, M., Easley, R., & Mathis, J. T. (2015). An automated procedure for laboratory and shipboard spectrophotometric measurements of seawater alkalinity: Continuously monitored single-step acid additions. *Marine Chemistry*, *174*, 141–146. doi: 10.1016/j.marchem.2015.06.008

Liu, X., Patsavas, M. C., & Byrne, R. H. (2011). Purification and characterization of meta-cresol purple for spectrophotometric seawater pH measurements. *Environmental Science and Technology*, *45*(11), 4862–4868. doi: 10.1021/es200665d

Lueker, T. J., Dickson, A. G., & Keeling, C. D. (2000). Ocean pCO_2 calculated from dissolved inorganic carbon, alkalinity, and equations for K1 and K2: validation based on laboratory measurements of CO_2 in gas and seawater at equilibrium. *Marine Chemistry, 70*(1–3), 105–119. doi: 10.1016/S0304-4203(00)00022-0

Lui, H. K., & Chen, C. T. A. (2017). Reconciliation of pH_{25} and pH_{insitu} acidification rates of the surface oceans: A simple conversion using only in situ temperature. *Limnology and Oceanography: Methods*, *15*(3), 328–335. doi: 10.1002/lom3.10170

Mehrbach, C., Culberson, C. H., Hawley, J. E., & Pytkowicx, R. M. (1973). Measurement of the apparent dissociation constants of carbonic acid in seawater at atmospheric pressure. *Limnology and Oceanography*, *18*(6), 897–907. doi: 10.4319/lo.1973.18.6.0897

Millero, F. J. (1979). The thermodynamics of the carbonate system in seawater. *Geochimica et Cosmochimica Acta, 43*(10), 1651–1661. doi: 10.1016/0016-7037(79)90184-4

Millero, F. J. (1995). Thermodynamics of the carbon dioxide system in the oceans. *Geochimica et Cosmochimica Acta, 59*(4), 661–677. doi: 10.1016/0016-7037(94)00354-O

Müller J. D., Rehder, G. (2018). Metrology of pH measurements in brackish waters–Part 2: Experimental characterization of purified meta-cresol purple for spectrophotometric pH_T measurements. *Frontiers in Marine Science, 5*. doi: 10.3389/fmars.2018.00177

Orr, J. C., Epitalon, J. M., Dickson, A. G., & Gattuso, J. P. (2018). Routine uncertainty propagation for the marine carbon dioxide system. *Marine Chemistry*, *207*(20), 84–107. doi: 10.1016/j.marchem.2018.10.006

Park, P. K. (1969). Oceanic CO_2 system: An evaluation of ten methods of investigation. *Limnology and Oceanography*, *14*(2), 179–186. doi: 10.4319/lo.1969.14.2.0179

Pegau, W. S., Gray, D., Ronald, J., & Zaneveld, V. (1997). Absorption and attenuation of visible and near-infrared light in water: dependence on temperature and salinity. *Appl. Opt. 36*, 6035–6046.

Roy, R. N., Roy, L. N., Vogel, K. M., Porter-Moore, C., Pearson, T., Good, C. E., Millero, F. J., & Campbell, D. M. (1993). The dissociation constants of carbonic acid in seawater at salinities 5 to 45 and temperatures 0 to 45°C. *Marine Chemistry, 44*(2–4), 249–267. doi: 10.1016/0304-4203(93)90207-5

Schockman, K. M., & Byrne, R. H. (2021). Spectrophotometric determination of the bicarbonate dissociation constant in seawater. *Geochimica et Cosmochimica Acta*, *300*(1), 231–245. doi: 10.1016/j.gca.2021.02.008

Sulpis, O., Lauvset, S. K., & Hagens, M. (2020). Current estimates of K1 * and K2 * appear inconsistent with measured CO2 system parameters in cold oceanic regions. *Ocean Science Discussions, 16*(4), 847–862. doi: 10.5194/os-2020-19

Waters, J. F., Millero, F. J., & Woosley, R. J. (2014). The free proton concentration scale for seawater pH. *Marine Chemistry*, *149*, 8–22. doi: 10.1016/j.marchem.2012.11.003

Whitfield, M., & Jagner, D. (1981). Marine electrochemistry: a practical introduction. *John Wiley and Sons*, Somerset, N. J. doi: 10.4319/lo.1983.28.5.1046

Woosley, R. J. (2021). Evaluation of the temperature dependence of dissociation constants for the marine carbon system using pH and certified reference materials. *Marine Chemistry*, *229*(20). doi: 10.1016/j.marchem.2020.103914

APPENDIX A: SUPPLEMENTARY INFORMATION

A.1 CO2sys Predictions

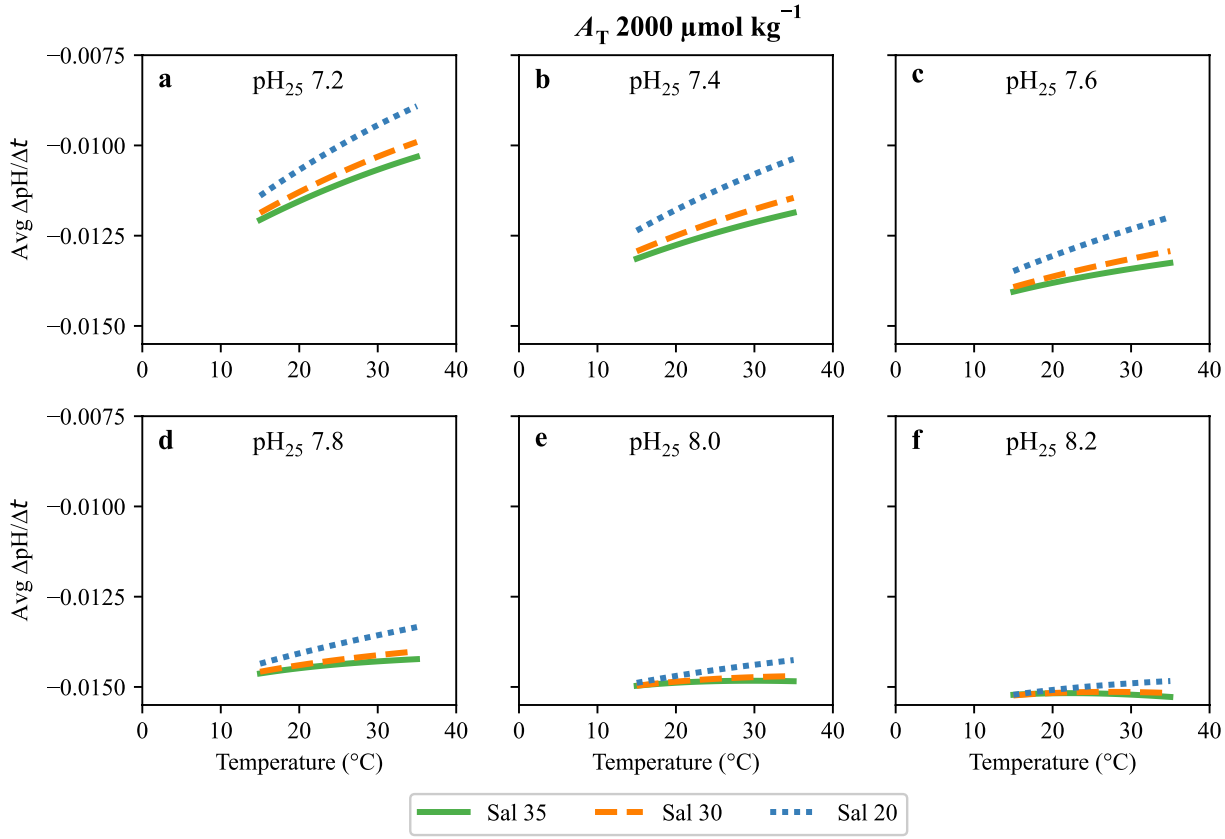

Figure A1: Averaged ΔpH/Δ*t* predictions of Lueker et al. (2000), Waters et al. (2014), and Schockman & Byrne (2021) models as a function of temperature. Averaged ΔpH/Δ*t* values are shown at salinities 20–35 and for pH_{25} values of 7.2 (a), 7.4 (b), 7.6 (c), 7.8 (d), 8.0 (e), and 8.2 (f). CO_2 system calculations were performed at A_T = 2000 µmol kg^{-1}.

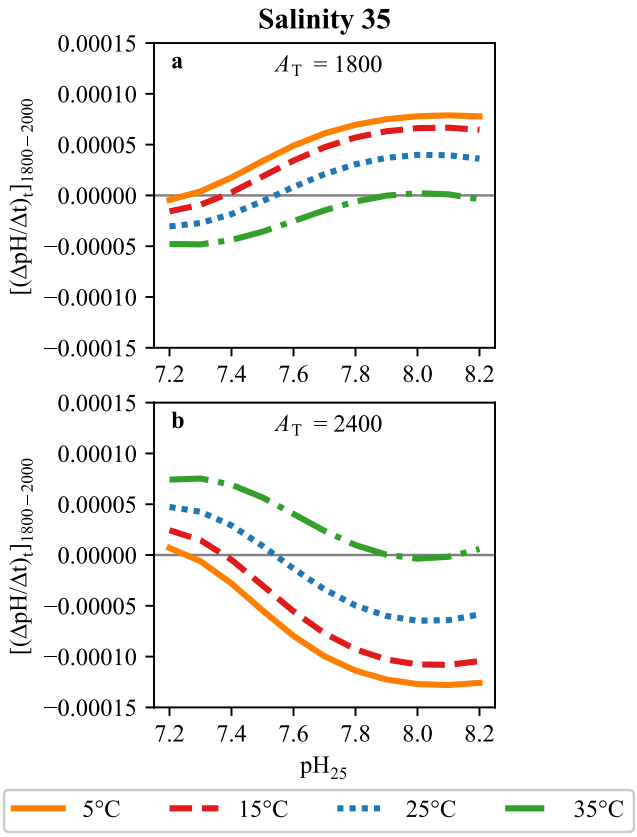

Figure A2: Residuals of $(\Delta pH/\Delta t)t$ calculated at an A_T of 1800 (a) and 2400 µmol kg^{-1} (b) relative to $(\Delta pH/\Delta t)_t$ at an A_T = 2000 µmol kg^{-1}. Calculations were performed at various reference temperatures (5, 15, 25, and 35°C) and at a salinity of 35. All calculations were performed with CO2sys using equilibrium constants of Lueker et al. (2000).

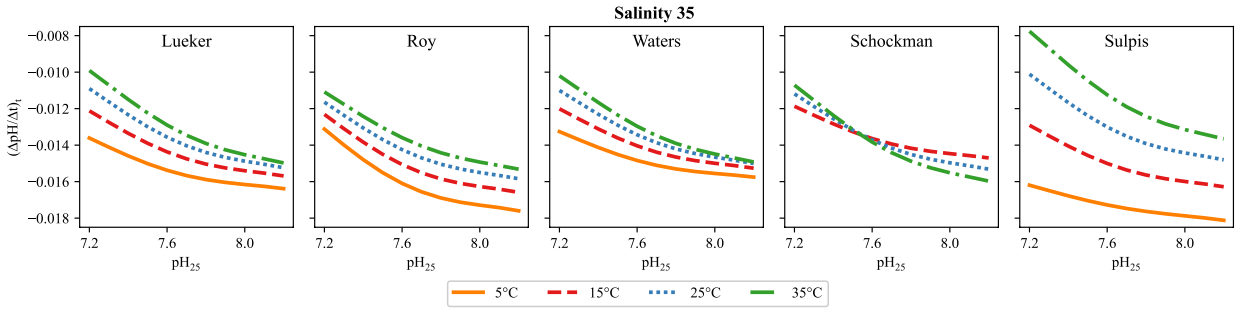

Figure A3: Determination of $(\Delta pH/\Delta t)_t$ at reference temperatures of 5, 15, 25, and 35°C for each equilibrium constant selection, where the calculation of $(\Delta pH/\Delta t)_5$ indicates the change in pH between temperatures 24.5 and 25.5°C. Calculations were performed using CO2sys at salinity = 35 and an A_T = 2000 µmol kg^{-1}.

A.2 Experimental Determinations of ΔpH/Δ*t*

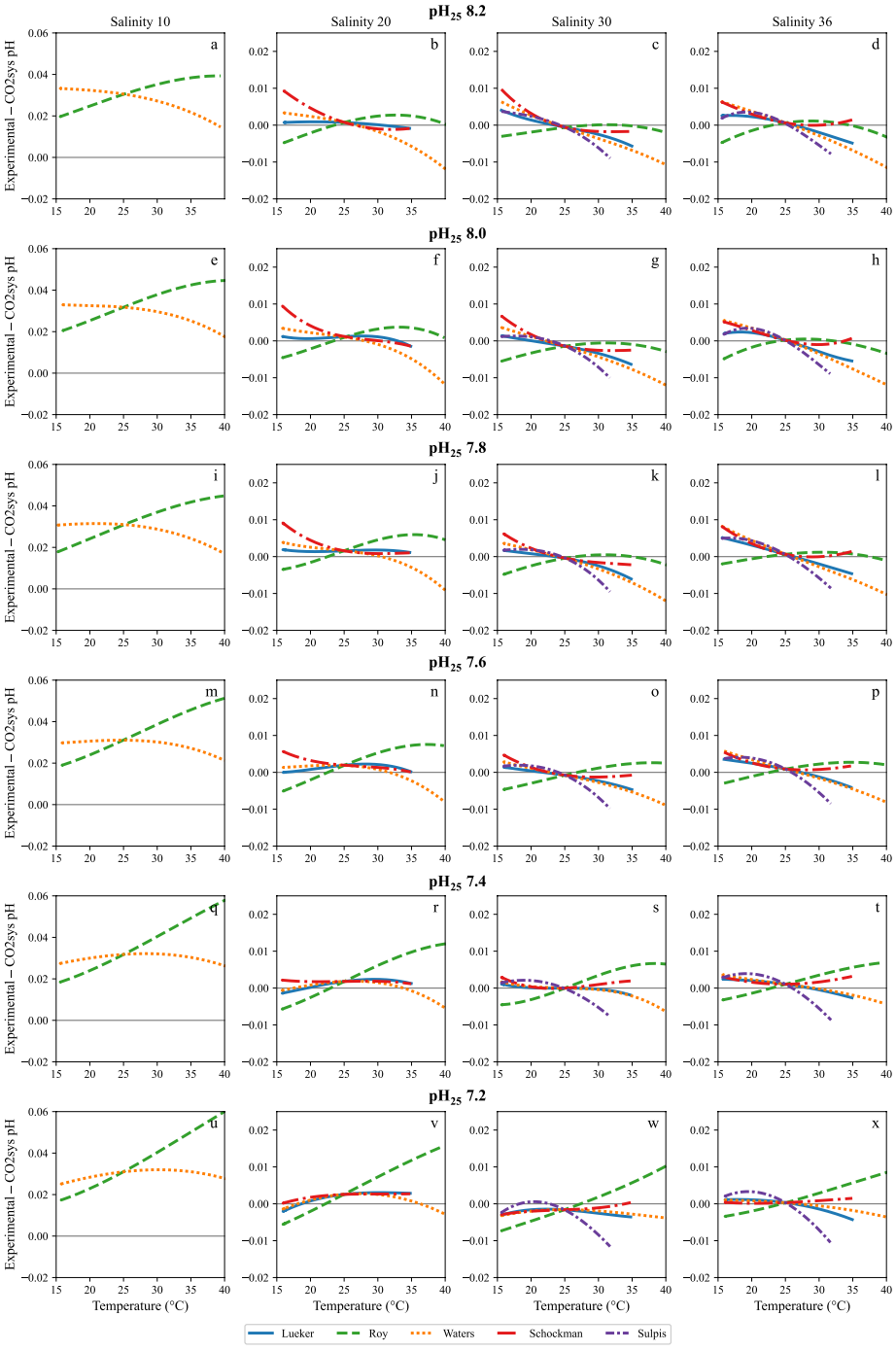

Figure A4: Consistency between experimental and CO2sys predicted pH at pH_{25} values of 8.2 (a–d), 8.0 (e–h), 7.8 (i–l), 7.6 (m–p), 7.4 (q–t), and 7.2 (u–x) and salinities of 10, 20, 30, and 36 (columns moving left to right). All CO2sys predictions were calculated using exact experimental temperature, pH_{25}, salinity, and A_T. A pH difference of zero is represented by solid black lines. Note, Sulpis et al. (2020) is defined for salinities 30.73–37.57, therefore calculations of Sulpis in (c, g, k, and o) are determined at a salinity of 30.73.

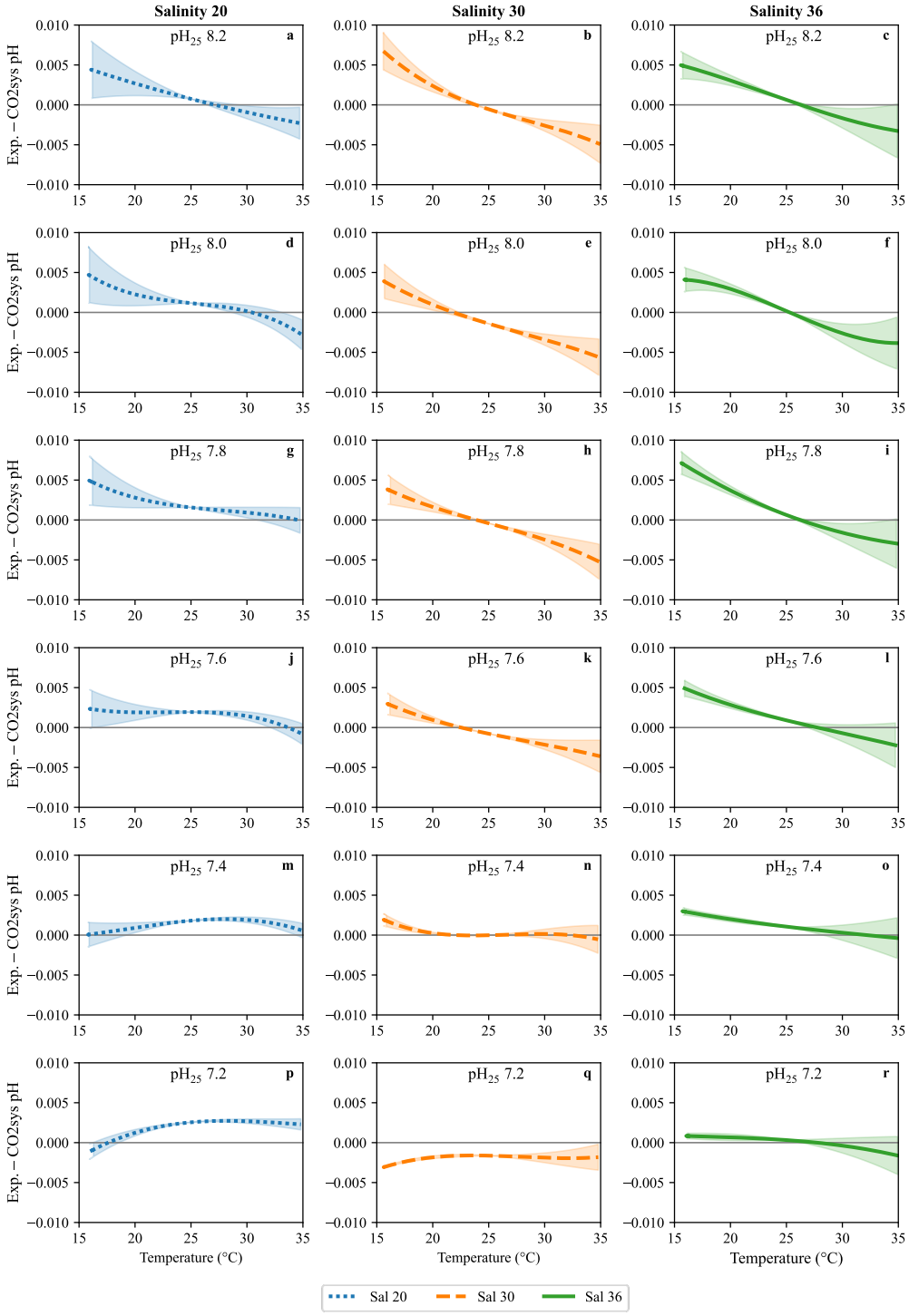

Figure A5: Difference between experimental and averaged CO2sys predictions of Lueker et al. (2000), Waters et al. (2014), and Schockman & Byrne (2021) models at pH_{25} values of 8.2 (a-c), 8.0 (d-f), 7.8 (g-i), 7.6 (j–l), 7.4 (m–o), and 7.2 (p–r) and salinities of 20 (left column), 30 (middle column), and 36 (right column). Shaded areas represent 1 standard deviation. All CO2sys predictions were calculated using exact experimental temperature, pH_{25}, salinity, and A_T. A pH difference of zero is represented by solid black lines.

A.3 Modeling ΔpH/Δ*t*

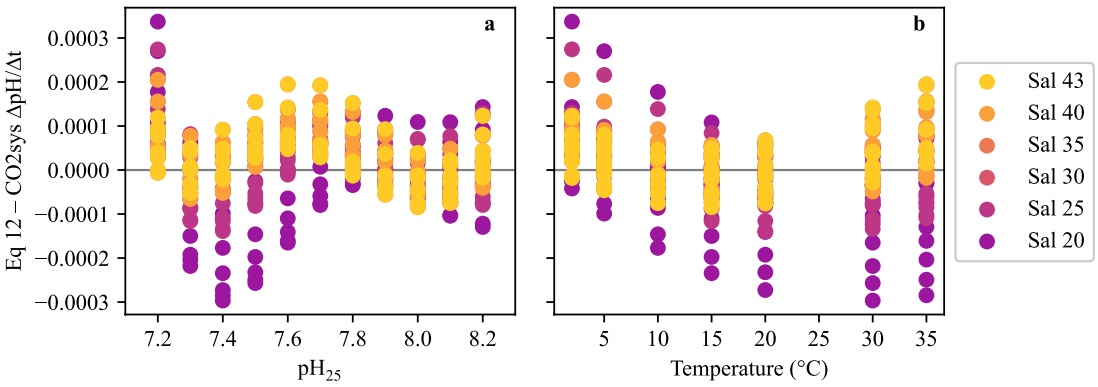

Figure A6: Residuals of modeled ΔpH/Δ*t* (Equation 12) and CO2sys predictions (constants from Lueker et al. (2000)) relative to pH_{25} (a), in-situ temperature (b), and salinity (marker colors).

Table A1: The standard deviation of Equation 12 residuals using two sets of coefficients at salinities 20–35. Coefficients were determined by fitting Equation 12 to experimental data (Table A2) and CO2sys generated data (constants from Lueker et al. 2000)(Table 2).

Salinity	Standard Deviation of Eq 12 Residuals	
	Exp Coefficients	CO2sys Coefficients
20	2.04×10^{-4}	9.84×10^{-5}
25	1.75×10^{-4}	6.32×10^{-5}
30	1.64×10^{-4}	6.02×10^{-5}
35	1.67×10^{-4}	8.34×10^{-5}

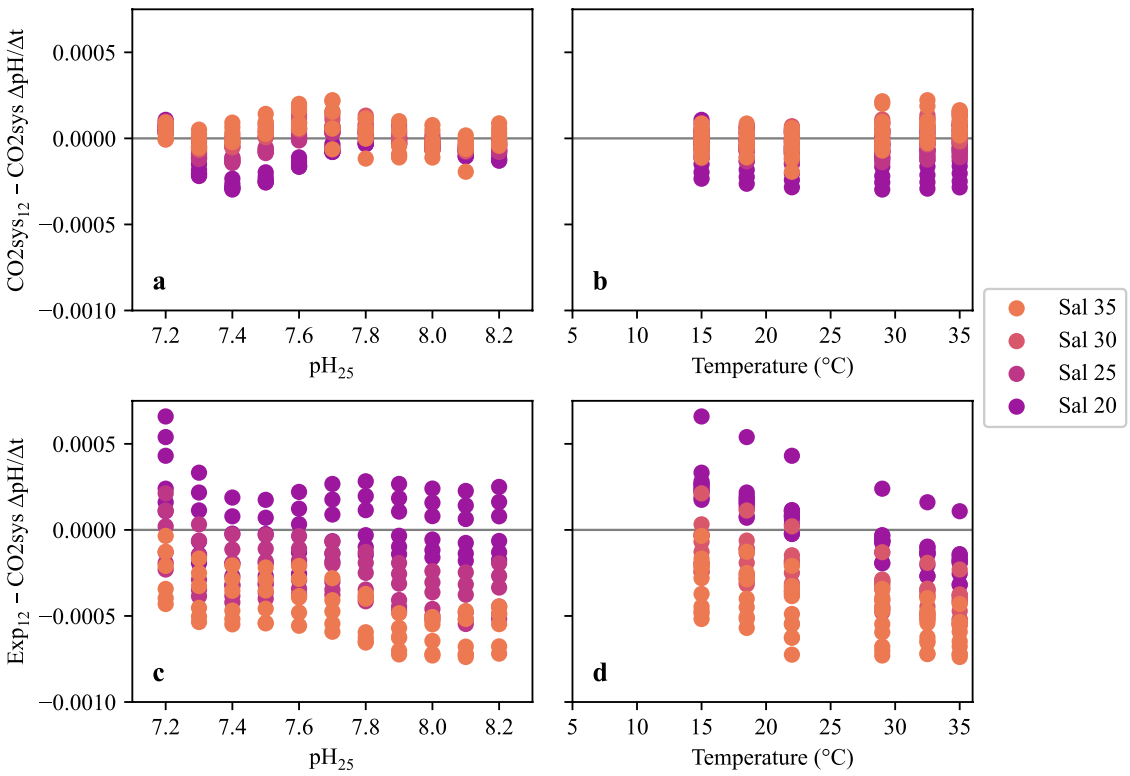

Figure A7: Residuals of ΔpH/Δ*t* calculated using two sets of coefficients for Equation 12 relative to CO2sys predictions. Coefficients for Equation 12 were found by fitting Equation 12 to CO2sys generated data (constants from Lueker et al. 2000; denoted as $CO2sys_{12}$, a–b) and by fitting Equation 12 to experimental data (denoted as Exp_{12}, c–d). Coefficients can be found in Tables 2 and A1 respectively. Residuals are shown relative to pH_{25} (a, c), temperature (b, d), and salinity (marker colors).

Equation A1 was fit to experimental data for salinities 10–36 and temperatures 15–40°C:

$$\begin{aligned} pH_{insitu} = \; & pH_{25} + (t - t_{25}) \cdot [a + b(pH_{25}) + c(pH_{25}^2) + d(pH_{25}^3) + e(t) + \\ & f(t \cdot pH_{25}) + g(t \cdot pH_{25}^2) + h(t \cdot pH_{25}^3) + i(t \cdot pH_{25}^4) + j(t^2 \cdot pH_{25}) \\ & k(S) + l(S \cdot pH_{25}) + m(S \cdot pH_{25}^2) + n(S \cdot pH_{25}^3) + o(S^2) \end{aligned} \tag{A1}$$

where t is the in-situ temperature (°C) and a–o are coefficients shown in Table A2 (Experimental). Residuals of Equation A1 relative to CO2sys prediction $\Delta pH/\Delta t$ values is shown in App. A, Figure A8.

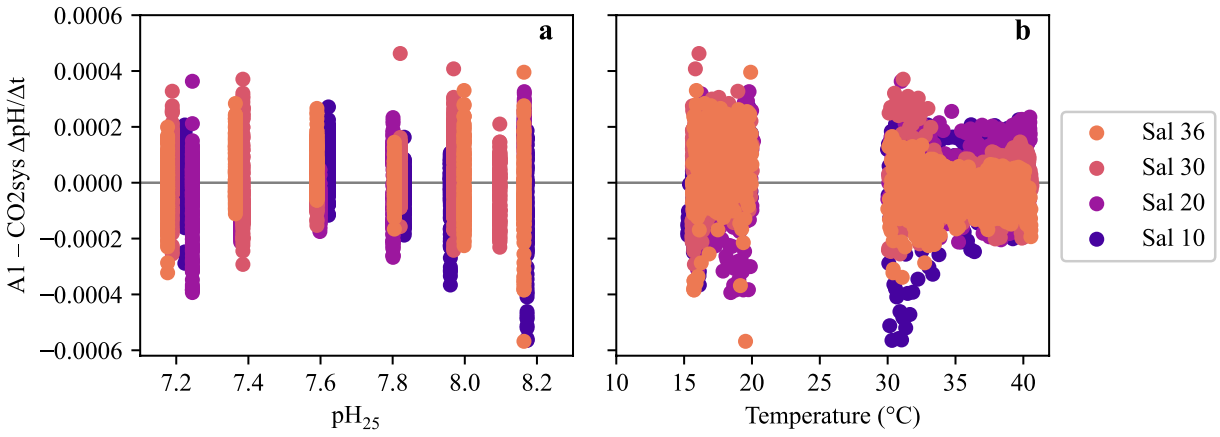

Figure A8: Residuals of $\Delta pH/\Delta t$ calculated using Equation A1 (coefficients in Table A2) relative to CO2sys predictions. Residuals are shown relative to pH_{25} (a), temperature (b), and salinity (marker colors).

Equation A2 was fit to CO2sys calculations of $\Delta pH/\Delta t$ using constants of Lueker et al. (2000) over the range of $19 < S < 43$ and $2 < t < 35$°C:

$$\begin{aligned} pH_{insitu} = \; & pH_{25} + (t - t_{25}) \cdot [a + b(pH_{25}) + c(pH_{25}^2) + d(pH_{25}^3) + e(t) + \\ & f(t \cdot pH_{25}) + g(t \cdot pH_{25}^2) + h(t \cdot pH_{25}^3) + i(t \cdot pH_{25}^4) + \\ & j(t^2) + k(t^2 \cdot pH_{25}) + l(t^2 \cdot pH_{25}^2) + m(t^2 \cdot pH_{25}^3) + n(t^2 \cdot pH_{25}^4) + \\ & o(S) + p(S \cdot pH_{25}) + q(S \cdot pH_{25}^2) + r(S \cdot pH_{25}^3) + s(S \cdot t \cdot pH_{25}) + \\ & t(S^2) + u(S^2 \cdot pH_{25}) + v(S^2 \cdot pH_{25}^2) \end{aligned} \tag{A2}$$

where t is the in-situ temperature (°C) and a–o are coefficients shown in Table A2 (Lueker et al. (2000) CO2sys). Residuals of Equation A2 relative to CO2sys prediction $\Delta pH/\Delta t$ values is shown in App. A, Figure A9.

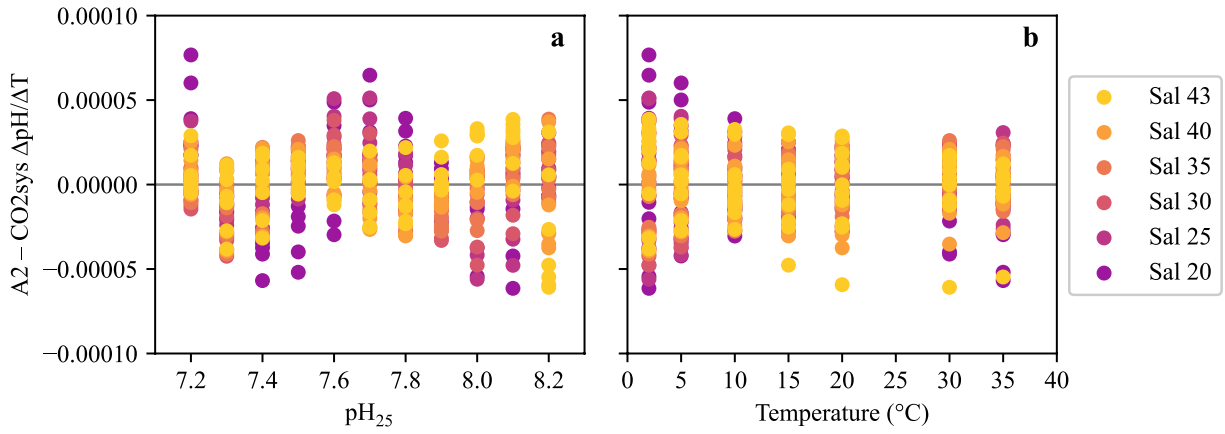

Figure A9: Residuals of $\Delta pH/\Delta t$ calculated using Equation A2 (coefficients in Table A2) relative to CO2sys predictions. Residuals are shown relative to pH_{25} (a), temperature (b), and salinity (marker colors).

Equation A3 was fit to CO2sys calculations of $\Delta pH/\Delta t$ using constants of Waters et al. (2014) over the range of $5 < S < 45$ and $0 < t < 45$°C:

$$\begin{aligned} pH_{insitu} = \; & pH_{25} + (t - t_{25}) \cdot [a + b(pH_{25}) + c(pH_{25}^2) + d(pH_{25}^3) + e(t) + \\ & f(t \cdot pH_{25}) + g(t \cdot pH_{25}^2) + h(t \cdot pH_{25}^3) + i(t \cdot pH_{25}^4) + \\ & j(t^2) + k(t^2 \cdot pH_{25}) + l(t^2 \cdot pH_{25}^2) + m(t^2 \cdot pH_{25}^3) + n(t^2 \cdot pH_{25}^4) + \\ & o(S) + p(S \cdot pH_{25}) + q(S \cdot pH_{25}^2) + r(S \cdot pH_{25}^3) + s(S \cdot t \cdot pH_{25}) + \\ & t(S^2) + u(S^2 \cdot pH_{25}) + v(S^2 \cdot pH_{25}^2) + w(S^2 \cdot t \cdot pH_{25}) + \\ & x(S^3) + y(S^4) \end{aligned} \tag{A3}$$

where t is the in-situ temperature (°C) and a–y are coefficients shown in Table A2 (Waters et al. (2014) CO2sys). Residuals of Equation A3 relative to CO2sys prediction $\Delta pH/\Delta t$ values is shown in Figure A10.

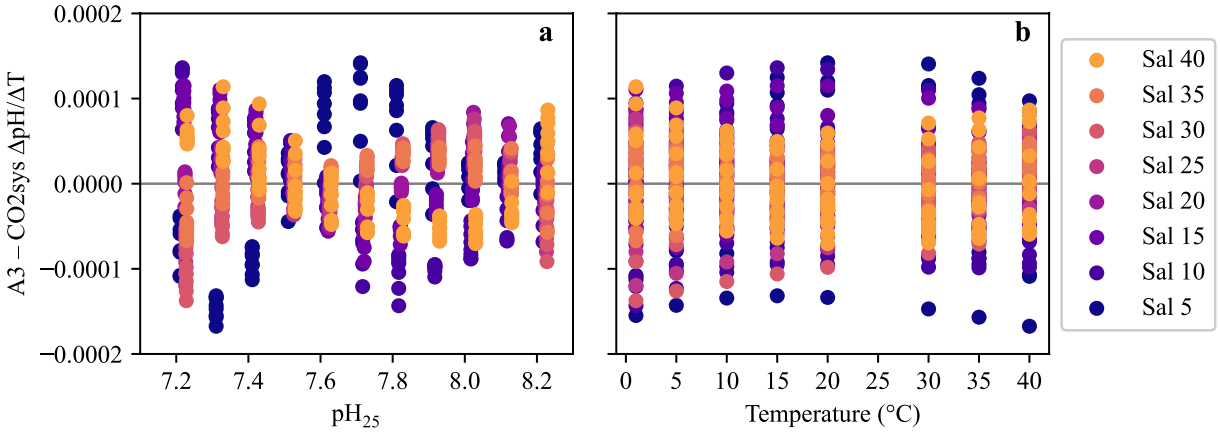

Figure A10: Residuals of $\Delta pH/\Delta t$ calculated using Equation A3 (coefficients in Table A2) relative to CO2sys predictions. Residuals are shown relative to pH_{25} (a), temperature (b), and salinity (marker colors).

Table A2: Coefficients for various models of $\Delta pH/\Delta t$ (Equations 12, A1-3) fit to experimental data (columns 1 and 2) and data generated in CO2sys using constants of Lueker et al. (2000) (column 3), and Waters et al. (2014) (column 4).

	Eq 12	**Eq A1**	**Eq A2**	**Eq A3**
	Experimental	**Experimental**	**Lueker et al. (2000) CO2sys**	**Waters et al. (2014) CO2sys**
a	0.26868	-1.5024	-2.8972	-2.8972
b	-0.06704	0.6069	1.14217	1.14217
c	0.003962	-0.081324	-0.14975	-0.14975
d	2.655×10^{-4}	3.5893×10^{-3}	6.5003×10^{-3}	6.5003×10^{-3}
e	-3.196×10^{-5}	-1.07397	-2.29625	-1.6984
f	-5.494×10^{-4}	0.551386	1.195675	0.84883
g	6.261×10^{-5}	-0.106046	-0.233251	-0.16362
h		9.0563×10^{-3}	0.0202052	0.014241
i		-2.8978×10^{-4}	-6.5579×10^{-4}	-4.6058×10^{-4}
j		-9.71×10^{-8}	0.0511473	0.032909
k		0.101456	-0.026647	-0.017081
l		-0.039187	5.20205×10^{-3}	3.3221×10^{-3}
m		0.0050239	-4.5099×10^{-4}	-2.8693×10^{-4}
n		-2.1402×10^{-4}	1.46506×10^{-5}	9.2859×10^{-6}
o		8.56×10^{-7}	0.10146231	0.13775
p			-0.0386066	-0.050529
q			4.86937×10^{-3}	6.1205×10^{-3}
r			-2.03629×10^{-4}	-2.4545×10^{-4}
s			-6.3246×10^{-8}	1.8143×10^{-6}
t			-1.3635×10^{-4}	-6.5718×10^{-7}
u			3.6492×10^{-5}	-4.5239×10^{-4}
v			-2.42646×10^{-6}	1.2226×10^{-4}
w				-7.8736×10^{-6}
x				8.4872×10^{-7}
y				-2.2364×10^{-7}
z				1.5083×10^{-8}
aa				1.2476×10^{-11}
bb				-4.5427×10^{-7}
cc				3.7052×10^{-9}